

PECULIARITIES OF SPECTRAL PARAMETERS OF EEG, HRV AND ROUTINE PARAMETERS OF IMMUNITY IN PATIENTS WITH VARIOUS LEVELS OF THE ENTROPY OF EEG, HRV, IMMUNOCYTOGRAM AND LEUKOCYTOGRAM

OO Popadynets¹, AI Gozhenko¹, W Zukow², IL Popovych^{3,1}

¹Ukrainian Scientific Research Institute of Medicine for Transport, Odesa
daddysbestmail@gmail.com

²Nicolaus Copernicus University, Torun², Poland zukow@umk.pl

³OO Bohomolets' Institute of Physiology, Kyiv i.popovych@biph.kiev.ua

Background. We have previously shown that the entropy levels of spectral parameters of EEG and HRV as well as of Immunocytogram and Leukocytogram are well dispersed. The method of cluster analysis was the distribution of the observed contingent into four groups that are homogeneous in terms of entropy. Have been identified the spectral parameters and indices of HRV, the amplitude-frequency and spectral parameters of the rhythms of EEG as well as the indices of asymmetry and lateralization of rhythms, which together are four clusters of entropy significantly different from each other. The **purpose** of this study is to identify the recognition parameters of immunity together with spectral parameters of EEG and HRV. **Material and methods.** In basal conditions in 37 men and 14 women with chronic pyelonephritis and cholecystitis in remission as well as without clinical diagnose but with dysfunction of neuro-endocrine-immune complex and metabolism, we recorded twice, before and after balneotherapy at the spa Truskavets', EEG ("NeuroCom Standard") and HRV ("Cardiolab+VSR"). In blood we determined parameters of Immune status on a set of I and II levels recommended by the WHO. Than we calculated for each locus of EEG and HRV as well as for Immunocytogram and Leukocytogram the Entropy (h) using Shannon's formula. **Results.** The cluster analysis method created four groups, homogeneous in entropy parameters. Discriminant analysis revealed 25 SPD of EEG parameters, 5 HRV parameters, and 9 immunity parameters, by the totality of which four entropy clusters clearly different from each other. **Conclusion.** Quantitatively and qualitatively different levels of entropy of the spectral parameters of EEG and HRV as well as the Immunocytogram and Leukocytogram are accompanied by characteristic constellations of the parameters of EEG, HRV and Immunity.

Keywords: EEG, HRV, Leukocytogram, Immunocytogram, Entropy, Clusters, Women and Man.

INTRODUCTION

We have previously shown that the entropy levels of spectral parameters of EEG and HRV as well as of Immunocytogram and Leukocytogram are well dispersed. The method of cluster analysis was the distribution of the observed contingent into four groups that are homogeneous in terms of entropy [23,24,38]. Have been identified the spectral parameters and indices of HRV, the amplitude-frequency and spectral parameters of the rhythms of EEG as well as the indices of asymmetry and lateralization of rhythms, which together are four clusters of entropy significantly different from each other [37]. We know about the relationships between the central and autonomic nervous and immune systems [1,5-7,9-12,14-17,19,21,25,30-35]. The **purpose** of this study is to identify the recognition parameters of immunity together with spectral parameters of EEG and HRV.

MATERIAL AND METHODS

The object of observation were 37 men and 14 women aged 23-76 years old, who came to the spa Truskavets' (Ukraine) for the treatment of chronic pyelonephritis and cholecystitis in remission as well as without clinical diagnose but with dysfunction of neuro-endocrine-immune complex and metabolism. The survey was conducted twice, before and after standard balneotherapy.

We recorded electrocardiogram in II lead (hardware-software complex "CardioLab+HRV" produced by "KhAI-MEDICA", Kharkiv, Ukraine) to assess the parameters of heart rate variability (HRV). For further analysis (Frequency Domain Methods) were selected spectral power (SP) bands of HRV: high-frequency (HF, range 0,4÷0,15 Hz), low-frequency (LF, range 0,15÷0,04 Hz), very low-frequency (VLF, range 0,04÷0,015 Hz) and ultra low-frequency (ULF, range 0,015÷0,003 Hz) [2,4,10].

Simultaneously we recorded EEG (hardware-software complex "NeuroCom Standard", KhAI Medica, Kharkiv, Ukraine) monopolar in 16 loci (Fp1, Fp2, F3, F4, F7, F8, C3, C4, T3, T4, P3, P4, T5, T6, O1, O2) by 10-20 international system, with the reference electrodes A and Ref on the tassels of ears. Among the options considered the average EEG amplitude (μV), average frequency (Hz), frequency deviation (Hz), index (%), coefficient of asymmetry (%) as well as absolute ($\mu\text{V}^2/\text{Hz}$) and relative (%) spectral power density (SPD) in the standard frequency bands: β (35÷13 Hz), α (13÷8 Hz), θ (8÷4 Hz) and δ (4÷0,5 Hz) in all loci, according to the instructions of the device.

In addition, we calculated Laterality Index (LI) for SPD each Rhythm using formula [20]:

$$\text{LI, \%} = \Sigma [200 \cdot (\text{Right} - \text{Left}) / (\text{Right} + \text{Left})] / 8$$

We calculated also for HRV and each locus EEG the Entropy (h) of normalized SPD using formula CE Shannon [26,29,36]:

$$\text{hHRV} = - [\text{SPDHF} \cdot \log_2 \text{SPDHF} + \text{SPDLF} \cdot \log_2 \text{SPDLF} + \text{SPDVLF} \cdot \log_2 \text{SPDVLF} + \text{SPDULF} \cdot \log_2 \text{SPDULF}] / \log_2 4;$$

$$\text{hEEG} = - [\text{SPD}\alpha \cdot \log_2 \text{SPD}\alpha + \text{SPD}\beta \cdot \log_2 \text{SPD}\beta + \text{SPD}\theta \cdot \log_2 \text{SPD}\theta + \text{SPD}\delta \cdot \log_2 \text{SPD}\delta] / \log_2 4$$

In portion of capillary blood we counted up Leukocytogram (LCG) (Eosinophils, Stub and Segmentonuclear Neutrophils, Lymphocytes and Monocytes) and calculated two variants of Adaptation Index as well as two variants of Strain Index by IL Popovych [3,22].

$$\text{Strain Index-1} = [(\text{Eo}/3,5-1)^2 + (\text{SN}/3,5-1)^2 + (\text{Mon}/5,5-1)^2 + (\text{Leu}/6-1)^2] / 4$$

$$\text{Strain Index-2} = [(\text{Eo}/2,75-1)^2 + (\text{SN}/4,25-1)^2 + (\text{Mon}/6-1)^2 + (\text{Leu}/5-1)^2] / 4$$

Immune status evaluated on a set of I and II levels recommended by the WHO as described in the manual [18]. For phenotyping subpopulations of lymphocytes used the methods of rosette formation with sheep erythrocytes on which adsorbed monoclonal antibodies against receptors CD3, CD4, CD8, CD22 and CD56 from company "Granum" (Kharkiv) with visualization under light microscope with immersion system. Subpopulation of T cells with receptors high affinity ("active" T Lymphocytes) determined by test of active rosette formation. The state of humoral immunity judged by the concentration in serum of Immunoglobulins classes G, A, M (ELISA, analyser "Immunochem", USA) and circulating immune complexes (by polyethylene glycol precipitation method).

We calculated also the Entropy (h) of Immunocytogram (ICG) and LCG using classical CE Shannon's formula [26,29,36]:

$$\text{hICG} = - [\text{CD4} \cdot \log_2 \text{CD4} + \text{CD8} \cdot \log_2 \text{CD8} + \text{CD22} \cdot \log_2 \text{CD22} + \text{CD16} \cdot \log_2 \text{CD16}] / \log_2 4$$

$$\text{hLCG} = - [\text{Lymph} \cdot \log_2 \text{Lymph} + \text{Mon} \cdot \log_2 \text{Mon} + \text{Eos} \cdot \log_2 \text{Eos} + \text{SNN} \cdot \log_2 \text{SNN} + \text{StubN} \cdot \log_2 \text{StubN}] / \log_2 5$$

Parameters of phagocytic function of neutrophils estimated as described by SD Douglas and PG Quie [8] with moderately modification by MM Kovbasnyuk [15]. The objects of phagocytosis served daily cultures of Staphylococcus aureus (ATCC N 25423 F49) as typical specimen for Gram-positive Bacteria and Escherichia coli (O55 K59) as typical representative of Gram-negative Bacteria. Both cultures obtained from Laboratory of Hydro-Geological Regime-Operational Station JSC “Truskavets’kurort”. Take into account the following parameters of phagocytosis: activity as percentage of neutrophils, in which found microbes - Hamburger’s Phagocytic Index; intensity as number of microbes absorbed one phagocytes - Microbial Count (MC) or Right’s Index; completeness as percentage of dead microbes - Killing Index (KI). Microbial number and index their digestion is determined for each phagocyte and fixed in phagocytic frame. Based of these parameters were calculated the Bactericidity of Neutrophils, contained in 1 L of blood, by formula:

$$\text{Bactericidity (10}^9 \text{ Bacteras/L)} = \text{Leuk(10}^9 \text{/L)} \cdot \text{Neutrophils (\%)} \cdot \text{PhI (\%)} \cdot \text{MC (B/Phag)} \cdot \text{KI (\%)} / 10^4$$

Results processed using the software package "Statistica 5.5".

RESULTS AND DISCUSSION

Based on the discriminant analysis by the forward stepwise method [13], 39 parameters are included in the model, in particular 9 parameters of the SPD of **delta**-and **theta**-rhythm, 3 parameters of **alpha**-rhythm, 4 parameters of **beta**-rhythm, 5 parameters of **HRV** as well as 9 parameters of **Immunity**. The remaining 19 immunity parameters were out of the model. In addition, 6 parameters of EEG and 3 parameters of HRV that are not formally included in the discriminatory model but are in fact recognizable are noteworthy (Tables 1 and 2).

Table 1. Discriminant Function Analysis Summary for Neuro-Immune Variables, their actual Levels for Clusters as well as Norm and Coefficients of Variability

Step 39, N of vars in model: 39; Grouping: 4 grps; Wilks' Λ : 0,0053; approx. $F_{(117)=7,3}$; $p < 10^{-6}$

VARIABLES CURRENTLY IN THE MODEL	Clusters of Entropy (n)				Parameters of Wilk's Statistics					Norm (88)	Cv
	IV (24)	III (9)	II (61)	I (8)	Wilks Λ	Par- tial Λ	F-re- move (3,6)	p- le- vel	Tole- ran- cy		
O2- δ SPD, $\mu V^2/Hz$	116	136	186	3071	,008	,640	11,3	10^{-5}	,252	94	1,063
F7- δ SPD, $\mu V^2/Hz$	92	453	134	3774	,008	,686	9,1	10^{-4}	,038	72	1,836
Fp2- δ SPD, $\mu V^2/Hz$	81	125	110	1992	,008	,663	10,2	10^{-4}	,020	110	2,162
F4- δ SPD, $\mu V^2/Hz$	115	152	196	651	,007	,734	7,2	10^{-3}	,058	89	0,994
Fp1- δ SPD, %	24	48	29	47	,006	,951	1,0	,386	,216	18,9	0,701
F7- δ SPD, %	33	55	35	58	,009	,599	13,4	10^{-5}	,165	25	0,786
Killing In St. aur, %	46,4	50,5	51,1	53,6	,006	,846	3,6	,018	,242	58,9	0,071
BC St. aur., 10^9 B/L	96	90	96	114	,006	,873	2,9	,041	,368	106	0,200
F7- θ SPD, %	12,0	8,9	8,7	2,0	,008	,706	8,3	10^{-4}	,370	7,6	0,564
T4- θ SPD, %	13,1	9,5	7,9	4,2	,007	,806	4,8	,005	,211	8,7	0,463
F4- θ SPD, %	16,0	5,0	9,1	4,9	,008	,663	10,2	10^{-4}	,080	10,3	0,424
P4- θ SPD, %	12,8	7,8	7,5	5,5	,006	,916	1,8	,152	,287	7,1	0,425
F3- θ SPD, %	15,3	5,6	11,2	6,2	,006	,902	2,2	,101	,161	9,2	0,400
F4- θ SPD, $\mu V^2/Hz$	76	31	40	29	,007	,754	6,5	10^{-3}	,054	39	0,630
VLF HRV SP, msec ²	1865	1163	1229	795	,006	,923	1,7	,185	,415	1397	0,578
Entropy of ICG	0,948	0,970	0,937	0,897	,006	,947	1,1	,349	,299	0,960	0,059
CD22 ⁺ B Lymph, %	24,5	24,1	23,7	22,5	,006	,920	1,7	,167	,509	20,0	0,175
CD3 ⁺ Tac Lymph, %	29,3	30,6	28,3	26,7	,006	,941	1,3	,296	,487	30,0	0,167
C4- δ SPD, %	30	61	31	31	,007	,735	7,2	10^{-3}	,153	22	0,525

F3-δ SPD, %	34	64	34	39	,007	,817	4,5	,007	,078	23	0,692
F4-δ SPD, %	30	60	37	43	,007	,753	6,6	10 ⁻³	,080	23	0,606
ULF HRV SP, %	3,4	11,2	4,0	5,5	,007	,736	7,2	10 ⁻³	,327	4,3	0,926
ULF HRV SP, msec²	98	218	151	152	,006	,852	3,5	,021	,220	122	1,021
CIC, units	35	43	34	40	,006	,900	2,2	,096	,545	45	0,389
Killing I E. coli, %	43,5	50,4	47,9	46,8	,006	,940	1,3	,292	,247	62,0	0,078
F3-β SPD, %	25,1	11,4	22,0	26,5	,007	,740	7,0	10 ⁻³	,094	26,3	0,609
T3-β SPD, %	32	15	29	16	,009	,612	12,7	10 ⁻⁵	,236	34	0,509
F4-β SPD, μV²/Hz	91	57	78	83	,008	,709	8,2	10 ⁻³	,135	76	0,443
T6-β SPD, μV²/Hz	78	47	76	133	,006	,849	3,6	,020	,432	92,5	0,839
Fp2-θ SPD, μV²/Hz	43	16	27	51	,006	,877	2,8	,048	,077	22	0,631
T6-θ SPD, μV²/Hz	38	16	28	26	,006	,922	1,7	,179	,219	17	0,642
P3-θ SPD, μV²/Hz	59	24	59	78	,007	,792	5,3	,003	,102	39	0,715
P4-α SPD, μV²/Hz	157	92	350	319	,006	,865	3,1	,032	,144	341	1,013
(VLF+LF)/HF	17	11,9	12,2	16,5	,006	,901	2,2	,099	,394	7,5	0,506
Monocytes, %	6,06	5,81	6,36	6,46	,006	,901	2,2	,097	,525	6,0	0,083
MC vs E. coli, M/Ph	67,1	57,6	64,3	62,0	,006	,949	1,1	,366	,596	54,7	0,097
O2-α SPD, %	35	27	50	26	,006	,828	4,1	,010	,170	54,5	0,453
Fp2-α SPD, %	28	20	35	16	,008	,636	11,5	10 ⁻⁵	,090	40	0,492
LF HRV SP, msec²	953	954	1089	623	,006	,942	1,2	,303	,406	640	0,529
VARIABLES CURRENTLY NOT IN THE MODEL	IV (24)	III (9)	II (61)	I (8)	Wilks Λ	Partial Λ	F to enter	p-level	Tolerance	Norm (88)	Cv
O2-δ SPD, %	28	39	26	55	,005	,961	,79	,503	,103	15	0,894
LF/HF	5,35	4,35	4,80	6,10	,005	,979	,42	,739	,171	2,76	0,675
Popovych's AI-1, pts	1,10	1,33	1,15	1,40	,007	,989	,23	,877	,470	1,70	0,147
Leukocytes, 10⁹/L	5,67	5,24	5,64	6,15	,007	,989	,23	,877	,264	5,00	0,100
BC E. coli, 10⁹ B/L	92	89	93	99	,007	,959	,86	,465	,069	99	0,200
CD56⁺ NK Lym, %	19,2	16,8	19,0	23,5	,007	,974	,54	,660	,102	17,0	0,172
θ Lymphocytes, %	1,1	-0,1	1,8	4,9	,007	,973	,54	,661	,104	0	0,576
T6-θ SPD, %	12,5	7,9	8,5	1,3	,007	,979	,43	,734	,344	6,5	0,477
CD8⁺ T-cytolytic, %	24,2	23,9	23,6	21,4	,007	,981	,40	,756	,261	23,5	0,138
Phag Ind St. aur., %	98,7	98,2	98,3	98,0	,007	,962	,78	,509	,499	98,3	0,018
C4-δ SPD, μV²/Hz	126	443	163	315	,007	,955	,95	,421	,136	87	0,792
SegN Neutrophils, %	54,7	58,2	52,4	53,3	,007	,991	,18	,910	,372	55,0	0,100
Stub Neutrophils, %	2,45	2,84	2,71	2,79	,007	,980	,42	,741	,564	4,25	0,147
CD4⁺ T-helpers, %	31,0	35,3	32,0	27,9	,005	,968	,66	,583	,224	39,5	0,082
Immunoglob A, g/L	1,73	2,00	1,73	1,59	,007	,978	,44	,722	,425	1,875	0,167
T5-β SPD, %	30	19	27	22	,005	,966	,69	,562	,192	37	0,618
C4-β SPD, %	26,1	14,1	23,4	24,9	,007	,968	,67	,573	,100	27,4	0,583
Fp1-β SPD, μV²/Hz	75	43	66	103	,007	,974	,52	,667	,197	66,5	0,484
Immunoglob M, g/L	1,51	1,36	1,46	1,41	,007	,968	,67	,573	,532	1,15	0,239
MC vs St. aur, M/Ph	65,0	57,6	62,5	61,8	,007	,975	,52	,669	,334	61,6	0,080
Pan Lymphocytes, %	33,8	30,3	35,1	34,0	,007	,992	,17	,918	,413	32,0	0,174
Entropy of LCG	0,644	0,637	0,661	0,669	,007	,992	,16	,925	,327	0,681	0,070
HF HRV SP, msec²	481	279	596	318	,005	,996	,08	,972	,119	347	1,358
Eosinophiles, %	2,97	2,90	3,46	3,31	,007	,987	,26	,851	,561	2,75	0,318
Popovych's SI-1, pts	0,21	0,15	0,23	0,12	,007	,961	,80	,498	,481	0,067	0,722
Popovych's SI-2, pts	0,25	0,16	0,30	0,18	,007	,973	,55	,650	,626	0,065	0,618
100•LF/(LF+HF), %	70,8	77,7	70,1	78,8	,005	,992	,15	,929	,262	66,3	0,210
Phag In vs E. coli, %	99,3	99,4	98,8	99,1	,005	,953	,98	,409	,482	98,3	0,012
Popovych's AI-2, pts	0,89	0,85	0,81	0,92	,007	,967	,68	,571	,627	1,70	0,147
Immunoglob G, g/L	14,8	14,4	14,2	15,0	,007	,967	,68	,568	,733	12,75	0,206

Table 2. Summary of Stepwise Analysis for Neuro-Immune Variables, ranked by criterion Lambda

Variables currently in the model	F to enter	p-level	Λ	F-value	p-level
O2- δ SPD, $\mu V^2/Hz$	22,5	10^{-6}	,593	22,5	10^{-6}
F4- θ SPD, %	16,7	10^{-6}	,391	19,4	10^{-6}
C4- δ SPD, %	10,3	10^{-5}	,296	16,9	10^{-6}
F7- δ SPD, $\mu V^2/Hz$	9,9	10^{-5}	,225	15,9	10^{-6}
ULF band HRV SP, %	9,0	10^{-4}	,175	15,3	10^{-6}
F3- β SPD, %	5,8	,001	,147	14,2	10^{-6}
T3- β SPD, %	4,4	,006	,129	13,1	10^{-6}
P4- θ SPD, %	3,3	,023	,116	12,1	10^{-6}
Fp2- δ SPD, $\mu V^2/Hz$	3,2	,026	,105	11,4	10^{-6}
F7- δ SPD, %	4,6	,005	,091	11,0	10^{-6}
F7- θ SPD, %	5,4	,002	,077	11,0	10^{-6}
F3- θ SPD, %	3,7	,014	,068	10,6	10^{-6}
Fp2- α SPD, %	3,5	,018	,060	10,3	10^{-6}
O2- α SPD, %	4,3	,007	,052	10,2	10^{-6}
T4- θ SPD, %	3,3	,024	,047	10,0	10^{-6}
Killing Index vs E. coli, %	3,3	,023	,042	9,8	10^{-6}
(VLF+LF)/HF as Centralization Index	2,9	,042	,038	9,6	10^{-6}
F4- δ SPD, %	2,7	,053	,034	9,4	10^{-6}
F4- δ SPD, $\mu V^2/Hz$	2,5	,067	,032	9,2	10^{-6}
P3- θ SPD, $\mu V^2/Hz$	4,3	,007	,027	9,3	10^{-6}
F3- δ SPD, %	3,5	,020	,024	9,2	10^{-6}
T6- β SPD, $\mu V^2/Hz$	3,1	,030	,021	9,2	10^{-6}
Fp2- θ SPD, $\mu V^2/Hz$	2,2	,095	,020	9,0	10^{-6}
Killing Index vs Staphylococ. aureus, %	2,7	,050	,018	8,9	10^{-6}
Bactericidity vs Staph. aur., 10^9 Bact/L	2,0	,123	,016	8,8	10^{-6}
F4- β SPD, $\mu V^2/Hz$	1,9	,135	,015	8,6	10^{-6}
F4- θ SPD, $\mu V^2/Hz$	6,3	10^{-3}	,012	9,0	10^{-6}
P4- α SPD, $\mu V^2/Hz$	3,0	,035	,011	9,0	10^{-6}
CD22 ⁺ B Lymphocytes, %	1,7	,183	,010	8,9	10^{-6}
CD3 ⁺ T Active Lymphocytes, %	1,6	,198	,009	8,7	10^{-6}
T6- θ SPD, $\mu V^2/Hz$	1,5	,227	,009	8,5	10^{-6}
Fp1- δ SPD, %	1,7	,169	,008	8,4	10^{-6}
Monocytes, %	1,4	,253	,008	8,2	10^{-6}
ULF band HRV SP, msec ²	1,3	,270	,007	8,1	10^{-6}
Circulating Immune Complexes, units	1,7	,173	,007	8,0	10^{-6}
LF band HRV SP, msec ²	1,5	,236	,006	7,8	10^{-6}
VLF band HRV SP, msec ²	1,2	,335	,006	7,7	10^{-6}
Entropy of Immunocytogram	1,0	,394	,006	7,5	10^{-6}
Microbial Count for E. coli, M/PhC	1,1	,366	,005	7,3	10^{-6}

Next, the 39-dimensional space of discriminant variables transforms into 3-dimensional space of a canonical roots. The canonical correlation coefficient is for Root 1 0,956 (Wilks' $\Lambda=0,005$; $\chi^2_{(117)}=416$; $p<10^{-6}$), for Root 2 0,906 (Wilks' $\Lambda=0,061$; $\chi^2_{(76)}=222$; $p<10^{-6}$), for Root 3 0,810 (Wilks' $\Lambda=0,344$; $\chi^2_{(37)}=85$; $p<10^{-5}$). The first root contains 61,8% of discriminative capabilities, the second 27,0% and the third 11,2%.

The calculation of the discriminant root values for each person as the sum of the products of raw coefficients to the individual values of discriminant variables together with the constant (Table 3) enables the visualization of each patient in the information space of the roots (Fig. 1).

Table 3. Standardized and Raw Coefficients and Constants for Neuro-Immune Variables

Coefficients	Standardized			Raw		
	Root 1	Root 2	Root 3	Root 1	Root 2	Root 3
Variables currently in the model	Root 1	Root 2	Root 3	Root 1	Root 2	Root 3
O2-δ SPD, $\mu V^2/Hz$	1,229	-,111	,239	,0013	-,0001	,0003
F4-θ SPD, %	-1,170	1,819	,604	-,2360	,3670	,1219
C4-δ SPD, %	-,128	-1,323	,644	-,0072	-,0745	,0363
F7-δ SPD, $\mu V^2/Hz$,911	-2,876	1,062	,0008	-,0024	,0009
ULF band HRV SP, %	-,602	-,755	-,102	-,1346	-,1688	-,0228
F3-β SPD, %	1,014	1,434	-,433	,0889	,1259	-,0380
T3-β SPD, %	-1,229	,372	-,484	-,0852	,0257	-,0336
P4-θ SPD, %	,310	-,129	,539	,0894	-,0373	,1552
Fp2-δ SPD, $\mu V^2/Hz$,490	4,279	-1,354	,0008	,0068	-,0022
F7-δ SPD, %	-1,409	,848	,172	-,0588	,0354	,0072
F7-θ SPD, %	-,805	-,387	,348	-,2135	-,1025	,0922
F3-θ SPD, %	,154	,066	-,943	,0294	,0126	-,1795
Fp2-α SPD, %	-1,282	1,751	-,225	-,0927	,1265	-,0163
O2-α SPD, %	,750	-,082	-,865	,0391	-,0043	-,0451
T4-θ SPD, %	-,934	,041	,427	-,2280	,0100	,1041
Killing Index vs E. coli, %	-,452	-,197	,192	-,0360	-,0157	,0153
(VLF+LF)/HF as Centralization Index	-,467	,222	,127	-,0347	,0165	,0095
F4-δ SPD, %	-,109	1,188	-1,703	-,0049	,0529	-,0759
F4-δ SPD, $\mu V^2/Hz$	-,619	-1,888	1,429	-,0019	-,0059	,0045
P3-θ SPD, $\mu V^2/Hz$	-,727	,936	-1,125	-,0115	,0148	-,0178
F3-δ SPD, %	,017	1,489	-,899	,0008	,0722	-,0436
T6-β SPD, $\mu V^2/Hz$,515	-,303	,220	,0068	-,0040	,0029
Fp2-θ SPD, $\mu V^2/Hz$	-,541	-1,159	,587	-,0153	-,0328	,0166
Killing Index vs Staphyl. aureus, %	-,158	-,343	-,887	-,0192	-,0416	-,1076
Bactericidity vs Staph. aur., 10^9 Bact/L	,173	,448	,484	,0071	,0182	,0197
F4-β SPD, $\mu V^2/Hz$	-1,167	,933	,546	-,0246	,0197	,0115
F4-θ SPD, $\mu V^2/Hz$	2,103	-,410	-,732	,0378	-,0074	-,0131
P4-α SPD, $\mu V^2/Hz$,763	-,693	-,149	,0029	-,0027	-,0006
CD22⁺ B Lymphocytes, %	-,139	,276	,344	-,0310	,0614	,0768
CD3⁺ T Active Lymphocytes, %	-,197	-,120	-,336	-,0395	-,0240	-,0674
T6-θ SPD, $\mu V^2/Hz$	-,127	,645	,014	-,0034	,0172	,0004
Fp1-δ SPD, %	-,145	,487	,135	-,0069	,0230	,0064
Monocytes, %	-,439	-,121	,035	-,1306	-,0361	,0104
ULF band HRV SP, msec²	,486	,680	,344	,0014	,0019	,0010
Circulating Immune Complexes, units	,312	,295	,184	,0205	,0194	,0121
LF band HRV SP, msec²	,073	-,059	-,456	,0001	-,0000	-,0003
VLF band HRV SP, msec²	-,344	-,247	,203	-,0002	-,0001	,0001
Entropy of Immunocytogram	-,314	-,317	,081	-5,9414	-5,9831	1,5312
Microbial Count vs E. coli, M/PhC	,244	,193	-,035	,0307	,0243	-,0044
			Constants	17,76	-9,413	4,855
			Eigenvalues	10,54	4,60	1,91
			Cumulative Properties	,618	,888	1,000

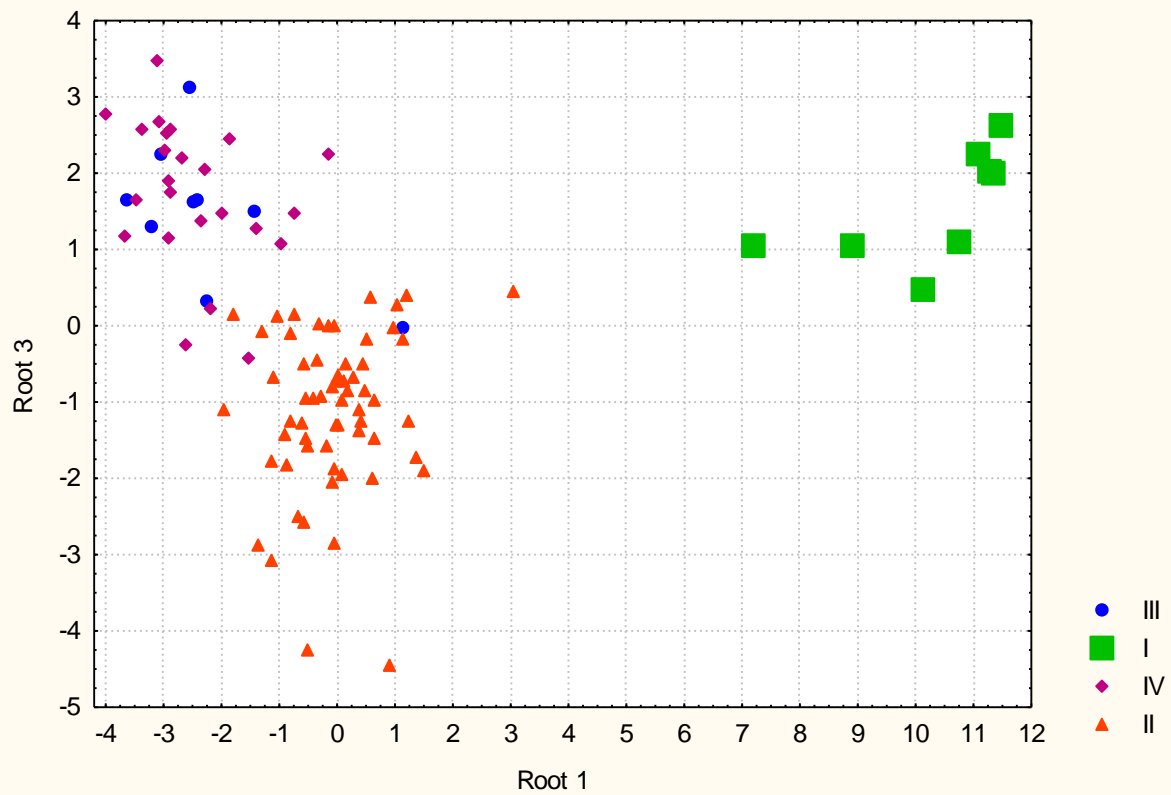
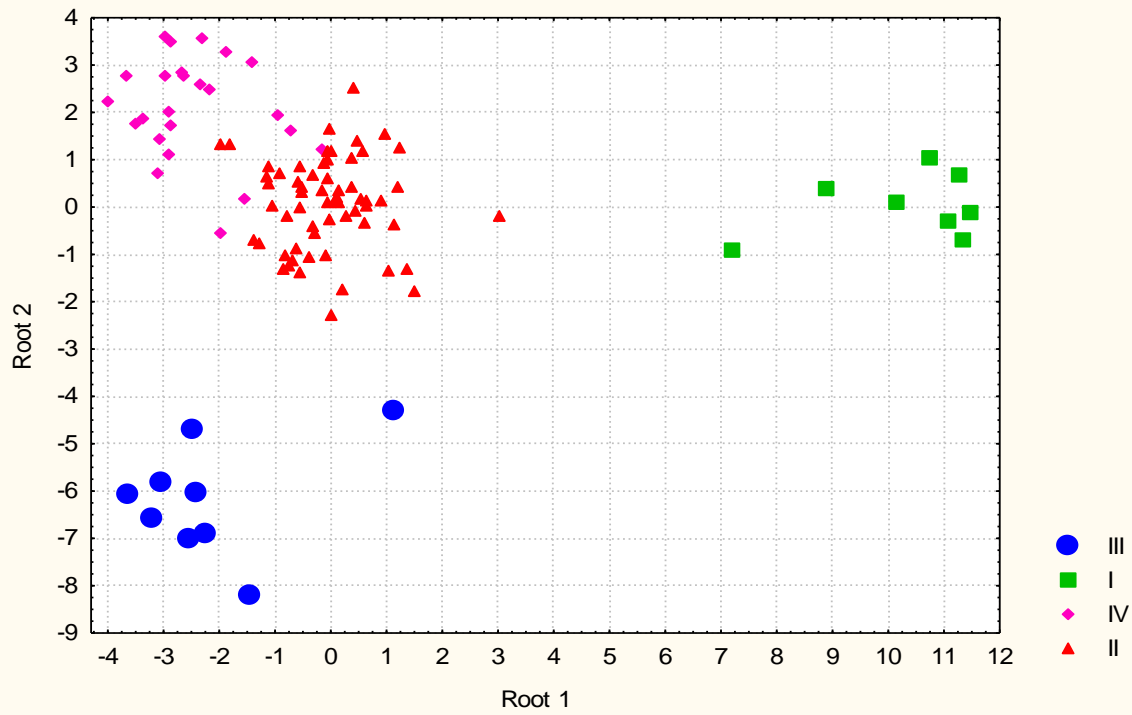


Fig. 1. Individual values of the neuro-immune discriminant roots of members of four entropy clusters

It is seen that all four clusters are fairly clearly delimited on the planes of the discriminant roots. The distinction after calculating root centroids becomes even clearer (Fig. 2). In particular, the first root dramatically the first cluster, the second - third and, to a lesser extent, the fourth clusters, and the third root distinguishes the second cluster. The visual impression is documented by the calculation of Mahalanobis distances between the centroids (Table 4).

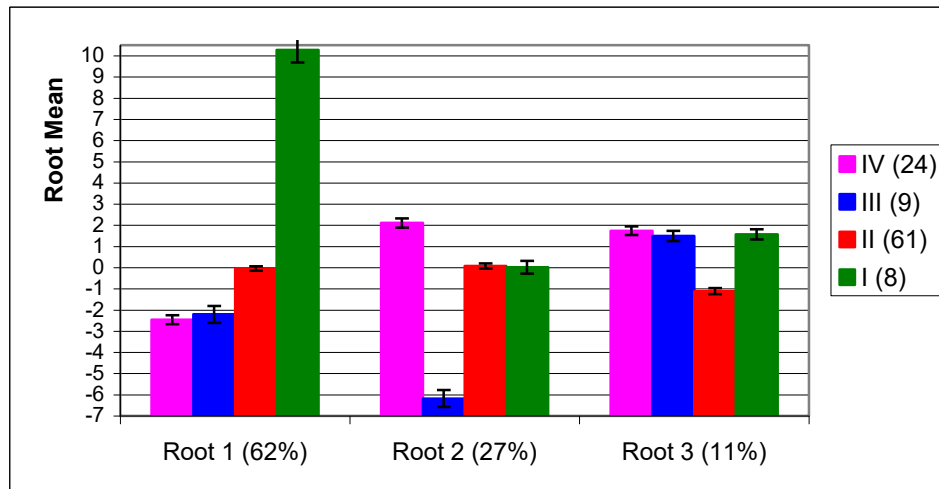


Fig. 2. Centroids of the neuro-immune discriminant roots of members of four entropy clusters

Table 4. Squared Mahalanobis Distances between Neuro-Immune Clusters and F-values (df=39,6; for all $p < 10^{-6}$)

Clusters	III	I	IV	II
III	0	202	72	53
I	11,8	0	173	118
IV	6,7	14,6	0	19
II	5,8	11,6	4,9	0

Table 5 presents the full structural coefficients and average values (centroids) of Roots as well as Z-scores of Variables.

Table 5. Correlations Variables-Canonical Roots, Means of Roots and Z-scores of Variables

Variables currently in the model	Root 1	Root 2	Root 3	IV (24)	III (9)	II (61)	I (8)
Root 1 (61,8%)				-2,46	-2,21	-0,05	+10,3
O2-δ SPD, $\mu V^2/Hz$,246	,000	,162	+0,22	+0,42	+0,92	+29,8
Fp2-δ SPD, $\mu V^2/Hz$,241	-,006	,171	-0,12	+0,06	0,00	+7,91
F7-δ SPD, $\mu V^2/Hz$,240	-,035	,192	+0,15	+2,88	+0,47	+28,0
F4-δ SPD, $\mu V^2/Hz$,112	-,126	,084	+0,30	+4,10	+1,21	+6,35
Fp1-δ SPD, %	,065	-,136	,067	+0,39	+2,17	+0,72	+2,12
F7-δ SPD, %	,063	-,108	,102	+0,43	+1,51	+0,48	+1,66
LF/HF	<i>Currently not in model</i>			+1,49	+1,21	+1,22	+2,63
Killing Index vs Staphyl. aureus, %	,058	-,055	-,111	-1,50	-1,00	-0,94	-0,63
Bactericidity vs Staph. aur., 10^9 Bac/L	,063	,029	,034	-0,95	-1,50	-0,96	+0,75
Popovych's Adaptation Index-1, pts	<i>Currently not in model</i>			-2,40	-1,49	-2,18	-1,19
Leukocytes, $10^9/L$	<i>Currently not in model</i>			+1,34	+0,48	+1,28	+2,29

Bactericidity vs E. coli, 10⁹ Bact/L	<i>Currently not in model</i>			-0,70	-0,96	-0,61	+0,03
CD56⁺ NK Lymphocytes, %	<i>Currently not in model</i>			+0,75	-0,07	+0,68	+2,20
0 Lymphocytes, %	<i>Currently not in model</i>			+0,20	-0,03	+0,32	+0,86
F7-0 SPD, %	-1,93	,090	,071	+1,02	+0,30	+0,26	-1,31
T4-0 SPD, %	-1,51	,093	,220	+1,08	+0,20	-0,19	-1,11
P4-0 SPD, %	-1,34	,161	,280	+1,88	+0,22	+0,12	-0,52
F4-0 SPD, %	-1,31	,260	,177	+1,31	-1,22	-0,28	-1,23
F3-0 SPD, %	-1,00	,217	,033	+1,64	-0,97	+0,53	-0,83
F4-0 SPD, $\mu V^2/Hz$	-0,49	,092	,104	+1,51	-0,32	+0,06	-0,39
VLF band HRV SP, msec²	-0,37	,046	,060	+0,58	-0,29	-0,21	-0,75
Entropy of Immunocytogram	-0,85	-,054	,040	-0,21	+0,18	-0,40	-1,12
CD3⁺ T Active Lymphocytes, %	-0,45	-,034	,054	-0,14	+0,11	-0,33	-0,65
CD22⁺ B Lymphocytes, %	-0,34	,010	,034	+1,30	+1,17	+1,04	+0,71
CD8⁺ T-cytolytic Lymphocytes, %	<i>Currently not in model</i>			+0,22	+0,12	+0,04	-0,66
Phagocytose Index vs Staph. aur., %	<i>Currently not in model</i>			+0,20	-0,02	+0,02	-0,14
Root 2 (27,0%)				+2,11	-6,18	+0,08	+0,02
C4-δ SPD, %	-,029	-2,14	,105	+0,75	+3,48	+0,79	+0,84
F3-δ SPD, %	-,007	-1,77	,104	+0,73	+2,63	+0,74	+1,08
F4-δ SPD, %	,020	-1,65	,014	+0,47	+2,67	+1,01	+1,43
ULF band HRV SP, %	,001	-2,14	,095	-0,24	+1,73	-0,08	+0,29
ULF HRV SP, msec²	,005	-0,41	-,019	-0,19	+0,77	+0,23	+0,24
Circulating Immune Complexes, units	,020	-0,65	,068	-0,59	-0,13	-0,60	-0,26
Killing Index vs E. coli, %	,009	-0,63	-,071	-1,91	-1,20	-1,45	-1,57
Segmentonuclear Neutrophils, %	<i>Currently not in model</i>			-0,06	+0,58	-0,48	-0,31
Stubnuclear Neutrophils, %	<i>Currently not in model</i>			-2,87	-2,26	-2,46	-2,33
CD4⁺ T-helper Lymphocytes, %	<i>Currently not in model</i>			-2,64	-1,29	-2,33	-3,59
Immunoglobulins A, g/L	<i>Currently not in model</i>			-0,47	+0,40	-0,48	-0,92
F3-β SPD, %	,034	,145	,019	-0,07	-0,93	-0,27	+0,01
T3-β SPD, %	-,064	,138	-,081	-0,13	-1,07	-0,27	-1,03
F4-β SPD, $\mu V^2/Hz$,002	,085	,034	+0,44	-0,57	+0,05	+0,21
T6-β SPD, $\mu V^2/Hz$,065	,049	,026	-0,19	-0,58	-0,22	+0,52
Fp2-0 SPD, $\mu V^2/Hz$,032	,090	,109	+1,53	-0,43	+0,39	+2,05
T6-0 SPD, $\mu V^2/Hz$	-,007	,070	,033	+1,82	-0,16	+0,94	+1,03
P3-0 SPD, $\mu V^2/Hz$,034	,067	-,016	+0,71	-0,53	+0,71	+1,38
P4-α SPD, $\mu V^2/Hz$,052	,039	-,218	-0,53	-0,72	+0,03	+0,06
(VLF+LF)/HF	,004	,042	,091	+2,25	+1,59	+1,63	+2,20
Microbial Count of E. coli, Micr/PhC	-,027	,144	-,000	+1,17	+0,27	+0,90	+0,69
Monocytes, %	,010	,010	-,030	+0,12	-0,38	+0,72	+0,92
Immunoglobulins M, g/L	<i>Currently not in model</i>			+1,31	+0,77	+1,11	+0,93
Microbial Count of Staph. aur., M/Ph	<i>Currently not in model</i>			+0,35	-0,40	+0,09	+0,02
Pan Lymphocytes, %	<i>Currently not in model</i>			+0,33	-0,31	+0,56	+0,36
Entropy of Leukocytogram	<i>Currently not in model</i>			-0,78	-0,92	-0,42	-0,25
Root 3 (11,2%)				+1,74	+1,49	-1,11	+1,57
O2-α SPD, %	-,035	,058	-,297	-0,77	-1,10	-0,20	-1,17
Fp2-α SPD, %	-,060	,069	-,264	-0,63	-1,00	-0,24	-1,24
LF band HRV SP, msec²	-,016	,001	-,044	+0,92	+0,92	+1,33	-0,05
HF band HRV SP, msec²	<i>Currently not in model</i>			+0,32	-0,22	+0,39	-0,17
Eosinophiles, %	<i>Currently not in model</i>			+0,25	+0,17	+0,82	+0,64
Popovych's Strain Index-1, points	<i>Currently not in model</i>			+2,71	+1,53	+3,20	+1,09
Popovych's Strain Index-2, points	<i>Currently not in model</i>			+4,51	+2,39	+5,83	+2,97
100•LF/(LF+HF), %	<i>Currently not in model</i>			+0,50	+1,07	+0,44	+1,12
Phagocytose Index vs E. coli, %	<i>Currently not in model</i>			+0,88	+0,90	+0,41	+0,70
Popovych's Adaptation Index-2, pts	<i>Currently not in model</i>			-3,24	-3,41	-3,56	-3,12
Immunoglobulins G, g/L	<i>Currently not in model</i>			+0,80	+0,62	+0,55	+0,84

The location of the variables in the composition of each root is carried out according to the algorithm of the traditional hierarchy of systems: central nervous, autonomic nervous, immune, which, however, is relatively conditional in light of current ideas about **bilateral** relationships between the three systems [5,6,21,32].

The localization of the members of the first cluster along the first root axis (Figs. 1 and 3) in the extreme right zone (centroide: +10,3) reflects **maximum** parameters of SPD of **δ -rhythm** as well as **LF/HF** ratio and **Immunity** which are related to the root **positively** (Table 5) as well as **minimum** for the sample parameters of SPD of **θ -rhythm**, **VLF** and other **Immune** which are related to the root **negatively** (Fig. 4).

Instead, the fourth cluster has an extreme left zone (centroide: -2,46), which reflects the **minimum/maximum** levels of these parameters. The members of the second cluster occupy an intermediate position (centroide: -0,05) while the centroide of the third cluster almost the same (-2,21) and their projections on the axis are mixed.

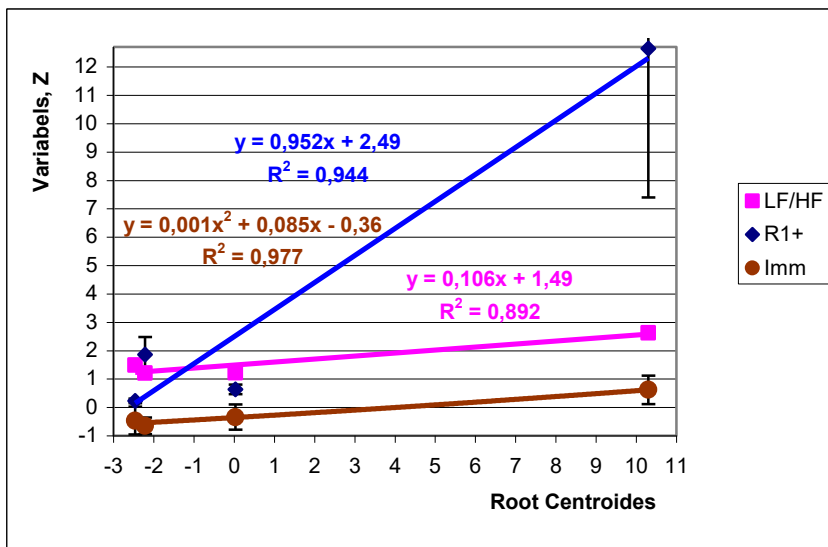


Fig. 3. Normalized values ($Z \pm SE$) of SPD of δ -rhythm, LF/HF and Immune parameters condensed in the first root that correlate with it positively

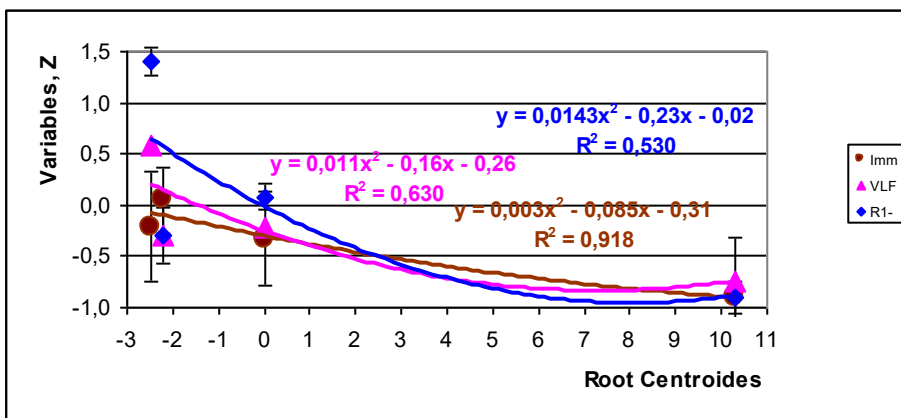


Fig. 4. Normalized values ($Z \pm SE$) of SPD of θ -rhythm, VLF and Immune parameters condensed in the first root that correlate with it negatively

A clear distinction between members of the third and fourth (as well as the second and first) clusters occurs along the axis of the second root (centroids: -6,18 vs +2,11; +0,08 and +0,02 respectively) (Table 5 and Fig. 1), which reflects the **maximum** for the sample levels of SPD of **δ -rhythm**, **ULF** and **Immune** parameters correlating **negatively** with root (Fig. 5), and **minimum** levels of SPD of **β -**, **θ -** and **α -rhythm**, **(VLF+LF)/HF** ratio and other **Immune** parameters correlating **positively** with root (Fig. 6).

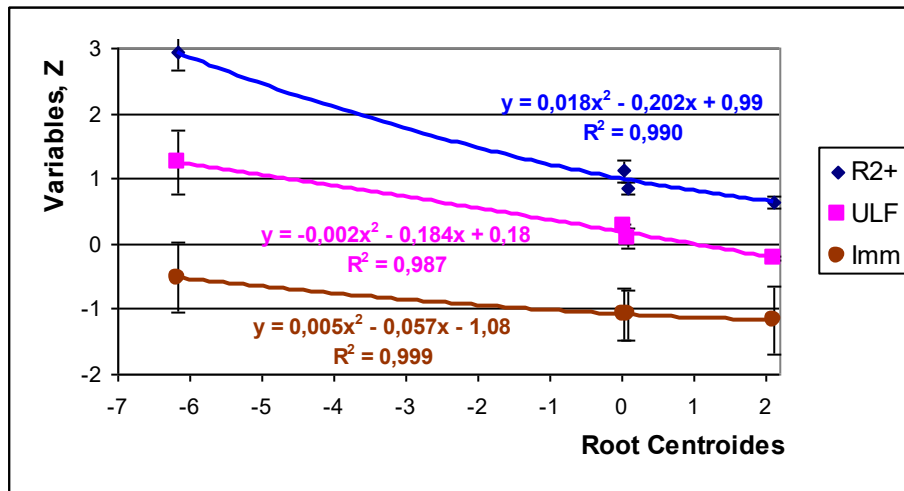


Fig. 5. Normalized values ($Z \pm SE$) of SPD of δ -rhythm, ULF and Immune parameters condensed in the second root that correlate with it negatively

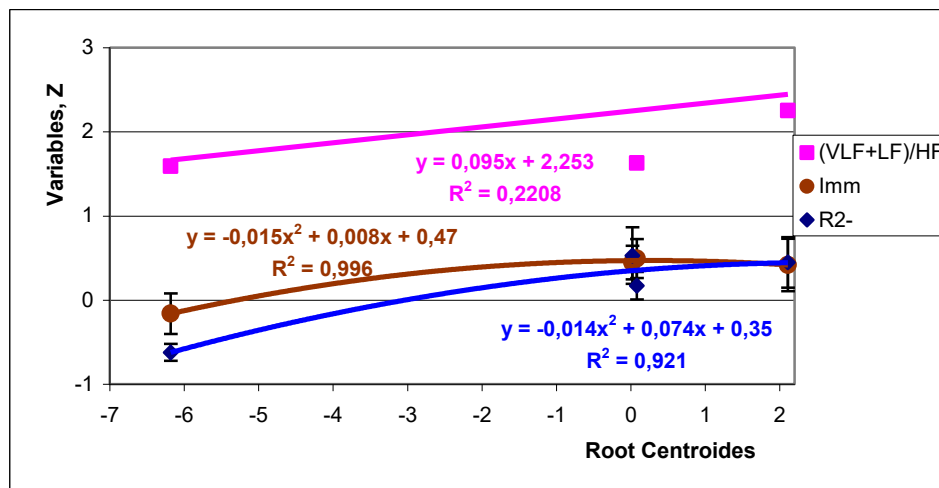


Fig. 6. Normalized values ($Z \pm SE$) of SPD of β -, θ - and α -rhythm, (VLF+LF)/HF and Immune parameters condensed in the second root that correlate with it positively

The members of the second cluster are distinguished from the other three also along the axis of the third root (centroids: -1,11 vs +1,74; +1,49 and +1,57) (Table 5 and Fig. 1), which reflects the **maximum** sampling levels of SPD of **α -rhythm**, **LF** and **HF** as well as **Immune** parameters that correlate **negatively** with the root (Fig. 7), and **minimum** for the sample levels of **LFnu** and others **Immune** parameters that correlate **positively** with the root (Fig. 8).

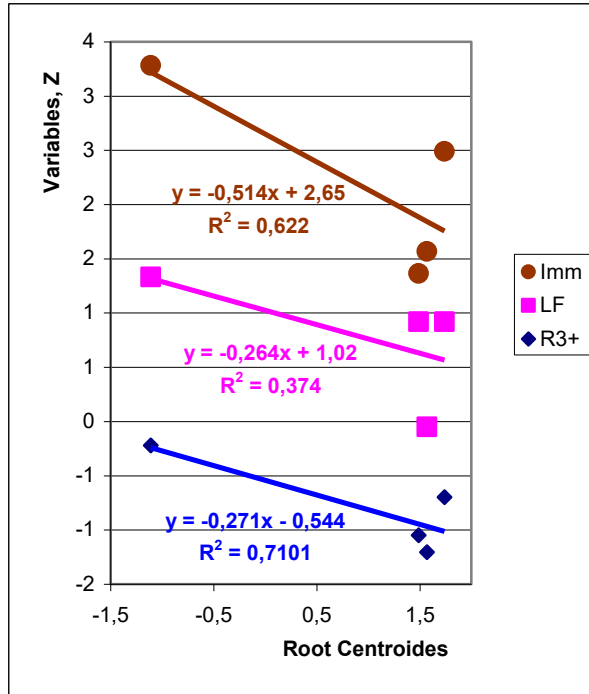


Fig. 7. Normalized values of **SPD of α -rhythm**, **HRV** and **Immune** parameters condensed in the third root that correlate with it negatively

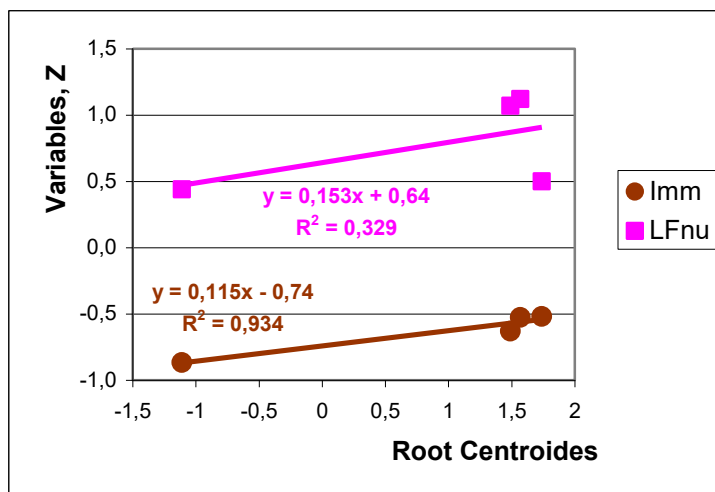


Fig. 8. Normalized values of **LFnu** and **Immune** parameters condensed in the third root that correlate with it positively

The same discriminant variables can be used to identify the belonging of one or another person to one or another cluster. This purpose of discriminant analysis is realized with the help of classifying functions (Table 6).

In this case, we can retrospectively recognize members of third and first clusters **unmistakably**, the second and fourth clusters are classified with one mistake. Overall classification accuracy is 98% .

Table 6. Coefficients and Constants for Classification Functions for Neuro-Immune Clusters

CLUSTERS	III	I	IV	II
Variables currently in the model	p=,088	p=,078	p=,235	p=,598
O2-δ SPD, $\mu V^2/Hz$	-,009	,006	-,010	-,008
F4-θ SPD, %	6,258	5,600	9,390	7,730
C4-δ SPD, %	-,730	-1,280	-1,337	-1,307
F7-δ SPD, $\mu V^2/Hz$	-,009	-,014	-,029	-,025
ULF band HRV SP, %	3,429	,700	2,058	2,141
F3-β SPD, %	2,157	4,044	3,168	3,236
T3-β SPD, %	1,625	,719	1,851	1,690
P4-θ SPD, %	-4,415	-3,518	-4,707	-4,858
Fp2-δ SPD, $\mu V^2/Hz$	-,027	,025	,029	,023
F7-δ SPD, %	1,495	,982	1,805	1,571
F7-θ SPD, %	5,143	1,851	4,371	3,801
F3-θ SPD, %	1,652	2,082	1,704	2,260
Fp2-α SPD, %	4,105	3,733	5,174	4,740
O2-α SPD, %	-,550	-,093	-,607	-,375
T4-θ SPD, %	6,149	3,375	6,316	5,450
Killing Index vs E. coli, %	,182	-,363	,065	-,033
(VLF+LF)/HF as Centralization Index	,441	,111	,589	,445
F4-δ SPD, %	,294	,556	,715	,812
F4-δ SPD, $\mu V^2/Hz$,045	-,015	-,002	-,007
P3-θ SPD, $\mu V^2/Hz$,272	,220	,394	,386
F3-δ SPD, %	1,725	2,179	2,312	2,292
T6-β SPD, $\mu V^2/Hz$	-,173	-,113	-,207	-,191
Fp2-θ SPD, $\mu V^2/Hz$	-,161	-,553	-,424	-,442
Killing Index vs Staphyloc. aureus, %	3,083	2,578	2,716	3,061
Bactericidity vs Staph. aur., 10^9 Bact/L	-,528	-,325	-,373	-,449
F4-β SPD, $\mu V^2/Hz$,439	,254	,611	,479
F4-θ SPD, $\mu V^2/Hz$	-,621	-,196	-,694	-,551
P4-α SPD, $\mu V^2/Hz$	-,062	-,042	-,085	-,071
CD22⁺ B Lymphocytes, %	-,750	-,750	-,214	-,632
CD3⁺ T Active Lymphocytes, %	-,389	-1,037	-,595	-,450
T6-θ SPD, $\mu V^2/Hz$,159	,224	,303	,259
Fp1-δ SPD, %	,852	,910	1,046	,965
Monocytes, %	5,787	3,935	5,523	5,252
ULF band HRV SP, msec²	-,058	-,028	-,042	-,045
Circulating Immune Complexes, units	-,676	-,299	-,517	-,542
LF band HRV SP, msec²	-,002	-,002	-,003	-,002
VLF band HRV SP, msec²	,004	,001	,003	,002
Entropy of Immunocytogram	765,4	654,3	717,7	711,
Microbial Count for E. coli, M/PhC	,455	,989	,647	,685
Constants	-671,7	-539,5	-736,1	-681,0

In conclusion, we consider it necessary to return to the KJ Tracey's [32] scheme of immunological homunculus (Fig. 9) by which the neural structures that are projected onto definite loci responsible for certain immune functions, that is the immune compartment cytokines release (F3 and/or F4), activation of memory B cells (Fp1 and/or Fp2), dendritic cells maturation (T3 and/T4), regulation of T cells (T5 and/or T6), clonal expansion (P3 and/or P4) and late cytokine release (P? or O?).

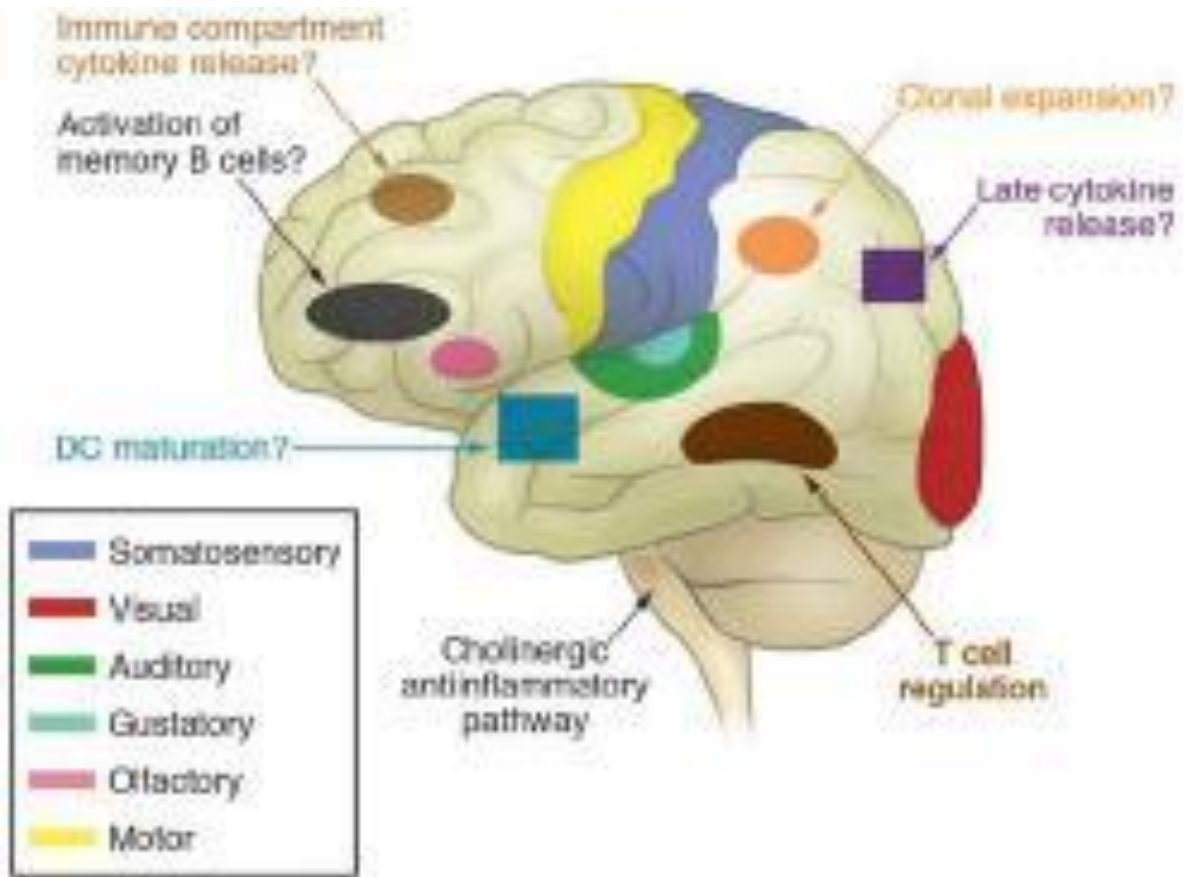


Fig. 9. KJ Tracey's scheme of immunological homunculus [0]

The data presented in Table 5 give us reason to bring to court colleagues, first and foremost from the Tracey's laboratory, our variant of immunological homunculus (Table 7), which contains not only EEG loci to which nerve structures are projected, but also the nature of the rhythm they generate.

Table 7. Our variant of immunological homunculus

Immune responses and EEG loci
Regulation of Phagocytosis?
NK Lymphocytes?
O2-δ
Fp2-δ
F7-δ
F4-δ
Fp1-δ
Regulation of T active and cytolytic and B Lymphocytes?
F7-θ
T4-θ
P4-θ

F4- θ
F3- θ
Regulation of Neutrophils, T helper Lymphocytes and IgA?
C4- δ
F3- δ
F4- δ
Regulation of Phagocytosis and IgM?
F3- β
T3- β
F4- β
T6- β
Fp2-
T6- θ
P3- θ
P4- α
Regulation of Eosinophils, Phagocytosis and IgG?
O2- α
Fp2- α

ACKNOWLEDGMENT

We express sincere gratitude to administration of JSC “Truskavets’kurort” and “Truskavets’ SPA” as well as clinical sanatorium “Moldova” for help in conducting this investigation.

ACCORDANCE TO ETHICS STANDARDS

Tests in patients are conducted in accordance with positions of Helsinki Declaration 1975, revised and complemented in 2002, and directive of National Committee on ethics of scientific researches. During realization of tests from all participants the informed consent is got and used all measures for providing of anonymity of participants.

For all authors any conflict of interests is absent.

References

1. Akmayev PG. Modern understanding of the interactions of regulatory systems: the nervous, endocrine and immune [in Russian]. *Uspekhi fiziologicheskikh nauk*. 1996; 27(1): 3-20.
2. Baevskiy RM, Ivanov GG. Heart Rate Variability: theoretical aspects and possibilities of clinical application [in Russian]. *Ultrazvukovaya i funktsionalnaya diagnostika*. 2001; 3: 106-127.
3. Barylyak LG., Malyuchkova RV, Tolstanov OB, Tymochko OB, Hryvna R, Uhryn MR. Comparative estimation of informativeness of leucocytary index of adaptation by Garkavi and by Popovych. *Medical Hydrology and Rehabilitation*. 2013; 11(1): 5-20.
4. Berntson GG, Bigger JT jr, Eckberg DL, Grossman P, Kaufman PG, Malik M, Nagaraja HN, Porges SW, Saul JP, Stone PH, Van der Molen MW. Heart Rate Variability: Origines, methods, and interpretive caveats. *Psychophysiology*. 1997; 34: 623-648.
5. Chavan SS, Pavlov VA, Tracey KJ. Mechanism and therapeutic relevance of neuro-immune communication. *Immunity*. 2017; 46: 927-942.
6. Chavan SS, Tracey KJ. Essential Neuroscience in Immunology. *J Immunol*. 2017; 198: 3389-3397.
7. Czura SJ, Tracey KJ. Autonomic neural regulation of immunity. *J Intern Med*. 2005; 257(2): 156-166.

8. Douglas SD, Quie PG. Investigation of Phagocytes in Disease. Churchill; 1981: 110 p.
9. Gozhenko AI, Hrytsak YL, Barylyak LG, Kovbasnyuk MM, Tkachuk SP, Korolyshyn TA, Matiyishyn GY, Zukow W, Popovych IL. Features of immunity by various constellations of principal adaptation hormones and autonomous regulation in practically healthy people. *Journal of Education, Health and Sport*. 2016; 6(10): 215-235.
10. Heart Rate Variability. Standards of Measurement, Physiological Interpretation, and Clinical Use. Task Force of ESC and NASPE. *Circulation*. 1996; 93(5): 1043-1065.
11. Hrytsak YaL, Barylyak LG, Zukow W, Popovych IL. Cluster analysis of hormonal constellation at women and men with harmonious and disharmonious general adaptation reactions. *Journal of Education, Health and Sport*. 2016; 6(4): 141-150.
12. Khaitov RM. Physiology of the Immune System [in Russian]. Moskwa. VINITI RAS; 2005: 428 p.
13. Klecka WR. Discriminant Analysis [trans. from English in Russian] (Seventh Printing, 1986). In: Factor, Discriminant and Cluster Analysis. Moskva: Finansy i Statistika; 1989: 78-138.
14. Kul'chyns'kyi AB, Gozhenko AI, Zukow W, Popovych IL. Neuro-immune relationships at patients with chronic pyelonephrite and cholecystite. Communication 3. Correlations between parameters EEG, HRV and Immunogram. *Journal of Education, Health and Sport*. 2017; 7(3): 53-71.
15. Kul'chyns'kyi AB, Kovbasnyuk MM, Korolyshyn TA, Kyjenko VM, Zukow W, Popovych IL. Neuro-immune relationships at patients with chronic pyelonephrite and cholecystite. Communication 2. Correlations between parameters EEG, HRV and Phagocytosis. *Journal of Education, Health and Sport*. 2016; 6(10): 377-401.
16. Kul'chyns'kyi AB, Kyjenko VM, Zukow W, Popovych IL. Causal neuro-immune relationships at patients with chronic pyelonephritis and cholecystitis. Correlations between parameters EEG, HRV and white blood cell count. *Open Medicine*. 2017; 12(1): 201-213.
17. Kul'chyns'kyi AB, Struk ZD, Gozhenko AI, Yanchij RI, Zukow WA, Kovbasnyuk MM, Korolyshyn TA, Popovych IL. Interrelations between changes in parameters of HRV, EEG and immunity. In: Materials of the XXth Congress of the Ukrainian Physiological Society named after PG Kostyuk. *Fiziol Zhurn*. 2019; 65(3). Suppl: 184-185.
18. Lapovets' LY, Lutsyk BD. Handbook of Laboratory Immunology [in Ukrainian]. Lviv. 2002. 173 p.
19. Nance DM, Sanders VM. Autonomic innervation and regulation of immune system (1987-2007). *Brain Behav Immun*. 2007; 21(6): 736-745.
20. Newberg AB, Alavi A, Baime M, Pourdehnad M, Santanna J, d'Aquili E. The measurement of regional cerebral blood flow during the complex cognitive task of meditation: a preliminary SPECT study. *Psychiatry Research: Neuroimaging Section*. 2001; 106: 113-122.
21. Pavlov VA, Chavan SS, Tracey KJ. Molecular and functional neuroscience in immunity. *Annu Rev Immunol*. 2018; 36: 783-812.
22. Petsyukh SV, Petsyukh MS, Kovbasnyuk MM, Barylyak LG, Zukow W. Relationships between Popovych's Adaptation Index and parameters of ongoing HRV and EEG in patients with chronic pyelonephrite and cholecystite in remission. *Journal of Education, Health and Sport*. 2016; 6(2): 99-110.
23. Popadynets' OO, Gozhenko AI, Zukow W, Popovych IL. Relationships between the entropies of EEG, HRV, immunocytogram and leukocytogram. *Journal of Education, Health and Sport*. 2019; 9(5): 651-666.
24. Popadynets' OO, Gozhenko AI, Zukow W, Popovych IL. Interpersonal differences between of the entropies of EEG, HRV, immunocytogram and leukocytogram. *Journal of Education, Health and Sport*. 2019; 9(6): 534-545.
25. Popovych IL. Feature of immunity by various constellations of hormones and autonomous regulation. In: Materials of the XXth Congress of the Ukrainian Physiological Society named after PG Kostyuk. *Fiziol Zhurn*. 2019; 65(3). Suppl: 184-184.
26. Popovych IL. Information effects of bioactive water Naftyssya in rats: modulation entropic, prevention desynchronizing and limitation of disharmonizing actions water immersion stress for

- information components of neuro-endocrine-immune system and metabolism, which correlates with gastroprotective effect [in Ukrainian]. *Medical Hydrology and Rehabilitation*. 2007; 5(3): 50-70.
27. Popovych IL, Kozyavkina OV, Kozyavkina NV, Korolyshyn TA, Lukovych YuS, Barylyak LG. Correlation between Indices of the Heart Rate Variability and Parameters of Ongoing EEG in Patients Suffering from Chronic Renal Pathology. *Neurophysiology*. 2014; 46(2): 139-148.
 28. Popovych IL, Lukovych YuS, Korolyshyn TA, Barylyak LG, Kovalska LB, Zukow W. Relationship between the parameters heart rate variability and background EEG activity in healthy men. *Journal of Health Sciences*. 2013; 3(4): 217-240.
 29. Shannon CE. Works on the theory of informatics and cybernetics [transl. from English to Russian]. Moskwa: Inostrannaya literatura; 1963: 329 p.
 30. Sternberg EM. Neural regulation of innate immunity: a coordinated nonspecific response to pathogens. *Nat Rev Immunol*. 2006; 6(4): 318-328.
 31. Thayer JF, Sternberg EM. Neural aspects of immunomodulation: Focus on the vagus nerve. *Brain Behav Immun*. 2010; 24(8): 1223-1228.
 32. Tracey KJ. Physiology and immunology of the cholinergic antiinflammatory pathway. *J Clin Invest*. 2007; 117(2): 289-296.
 33. Tracey KJ. Understanding immunity requires more than immunology. *Nature Immunology*. 2010; 11(7): 561-564.
 34. Winkelmann T, Thayer JF, Pohlak ST, Nees F, Grimm O, Flor H. Structural brain correlates of heart rate variability in healthy young adult population. *Brain Structure and Function*. 2017; 222(2): 1061-1068.
 35. Yoo HJ, Thayer JF, Greenig S, Lee TH., Ponzio A, Min J, Sakaki M, Nga L, Mater M, Koenig J. Brain structural concomitants of resting state heart rate variability in the young and old: evidence from two independent samples. *Brain Structure and Function*. 2018; 223(2): 727-737.
 36. Yushkovs'ka OG. Using information theory to study adaptive responses in the body athletes [in Ukrainian]. *Medical Rehabilitation, Kurortology, Physiotherapy*. 2001; 1(25): 40-43.
 37. Zukow W, Popadynets' OO, Gozhenko AI, Popovych IL.. Interindividual differences in parameters of the EEG and HRV in the humans with various levels of the entropy of EEG, HRV, immunocytogram and leukocytogram. *Journal of Education, Health and Sport*. 2019; 9(7): 448-466.
 38. Zukow W, Popadynets' OO, Gozhenko AI, Popovych IL. Interrelationships between the entropy of EEG, HRV, immunocytogram and leukocytogram in former sportsmen with chronic pyelonephritis and cholecystitis in remission. In: *Research in sports science insid social sciences framework Costa Blanca Sports Science Events*. *Journal of Human Sport and Exercise*. 2019; 14: **1-10**.